運輸省港湾技術研究所

港湾技術研究所報告

REPORT OF THE PORT AND HARBOUR RESEARCH INSTITUTE

MINISTRY OF TRANSPORT

VOL. 29 NO. 4 DEC. 1990

NAGASE, YOKOSUKA, JAPAN

港湾技術研究所報告 (REPORT OF P.H.R.I.)

第29巻　第4号 (Vol. 29, No. 4) 1990年12月 (Dec. 1990)

目　　次 (CONTENTS)

REPORT OF THE PORT AND
HARBOUR RESEARCH INSTITUTE
Vol. 29, No. 4 (Dec. 1990)

3. Parameter Identification for a Cyclic Mobility Model

Susumu IAI*
Yasuo MATSUNAGA**
Tomohiro KAMEOKA**

Synopsis

Within the framework of strain space plasticity approach for cyclic mobility (Iai et al,. 1990), this paper shows how to represent the realistic hysteretic damping factor under cyclic loading. In the present approach, actual cyclic shear mechanism is decomposed into a set of one dimensional virtual simple shear mechanisms. Four parameters defining the virtual simple shear mechanism under cyclic loading condition are identified with the soil parameters measured by the cyclic simple shear test.

The paper also shows how to identify the rest of five parameters defining the cumulative volumetric strain of plastic nature for representing cyclic mobility. The undrained cyclic test results, which are commonly available in the practice of soil dynamics and earthquake engineering, are fully utilized for the parameter identification.

Key words: constitutive equation of soil, dynamic, earthquake, liquefaction, plasticity, sand

* Chief of Geotechnical Earthquake Engineering Laboratory, Structural Engineering Division
** Member of Geotechnical Earthquake Engineering Laboratory, Structural Engineering Division

港湾技術研究所報告
第29巻 第4号 (1990.12)

3. サイクリックモビリティーのモデルのパラメータの同定

井合 進*・松永康男**・亀岡知弘**

要 旨

本研究では，同著者によるひずみ空間における塑性論に基づくサイクリックモビリティーのモデルの枠組みの中で，排水状態での土の繰り返しせん断における履歴減衰を忠実にモデル化するための方法を提案した。モデルの枠組みは，実際の土のせん断挙動を複数の一次元的かつ仮想的な単純せん断の機構に分解するものである。提案モデルでは，繰り返しせん断における仮想的な単純せん断の機構が4つのパラメータで規定されるが，これらのパラメータは繰り返しせん断において実際に測定し得る土のパラメータにより決定される。

本モデルでは，さらに，サイクリックモビリティーを表現するための塑性的な累積体積ひずみを規定するため5つのパラメータが用いられているが，これらのパラメータの決定方法も示した。土質動力学および地震工学においては，非排水条件での繰り返しせん断試験が実施されることが一般であることを考慮し，これらのパラメータを非排水条件での繰り返しせん断試験の結果から決定する方法を示している。

キーワード：液状化／構成式／地震／砂／塑性論／動的

* 構造部地盤震動研究室長
** 構造部地盤震動研究室

CONTENTS

1. Introduction

Cyclic mobility of saturated cohesionless soil during earthquakes causes limited, but often large, amount of deformation in soil structures and foundations. In practice, cyclic mobility occurring in the looser cohesionless soil is often called 'liquefaction,' which is distinguished from the 'cyclic mobility' occurring in the denser cohesionless soil. In the present paper, both phenomena will be called cyclic mobility as long as the mechanism does not involve the flow failure of soil. For estimating the amount of deformation, a simple but realistic modeling of cyclic mobility is essential. In particular, the reasonable representation is needed of hysteretic damping factor during cyclic loading. In the previous study, the framework is offered based on the strain space plasticity approach (Iai et al., 1990). Explicit modeling of hysteresis loop is yet to be given by specifying memory of loading history and unloading/reloading functions.

Reasonable identification of model parameters with the laboratory test results is also important for estimating the damage due to cyclic mobility. Though the triaxial compression tests under drained condition are often considered as a basis for identifying all the model parameters, this is not the case in the practice of soil dynamics and earthquake engineering; the undrained cyclic loading tests are considered as a basis for analyzing seismic performance of soil structures and foundations. Therefore, a procedure is needed for identifying the model parameters by fully utilizing the undrained cyclic loading test results.

The aim of the present study is to establish the modeling of realistic hysteretic damping factor and to show the reasonable identification procedure of model parameters within the framework of strain space plasticity approach for cyclic mobility.

2. Basic Equations

2.1 Constitutive Relation

Cyclic mobility under plane strain condition is represented as the relation between the effective stress and the strain given by

$$\boldsymbol{\sigma}'^{T}=(\sigma_x', \sigma_y', \tau_{xy}) \tag{1}$$

$$\boldsymbol{\varepsilon}^{T}=(\varepsilon_x, \varepsilon_y, \gamma_{xy}) \tag{2}$$

in which compressive stress and contractive strain will be assumed negative. Within the framework of strain space plasticity approach, the incremental constitutive relation is given by $I+1$ separate mechanisms for $i=0, \cdots\cdots, I$ as (Iai et al., 1990)

$$d\boldsymbol{\sigma}'=K\boldsymbol{n}^{(0)}\boldsymbol{n}^{(0)T}(d\boldsymbol{\varepsilon}-d\boldsymbol{\varepsilon}_p)+\sum_{i=1}^{I}R_{L/U}{}^{(i)}\boldsymbol{n}^{(i)}\boldsymbol{n}^{(i)T}d\boldsymbol{\varepsilon} \tag{3}$$

in which the volumetric strain increment $d\boldsymbol{\varepsilon}_p$ of plastic nature is given by

$$d\boldsymbol{\varepsilon}_p{}^{T}=d(\varepsilon_p/2, \varepsilon_p/2, 0) \tag{4}$$

and the direction vectors $\boldsymbol{n}^{(i)}$ are given by

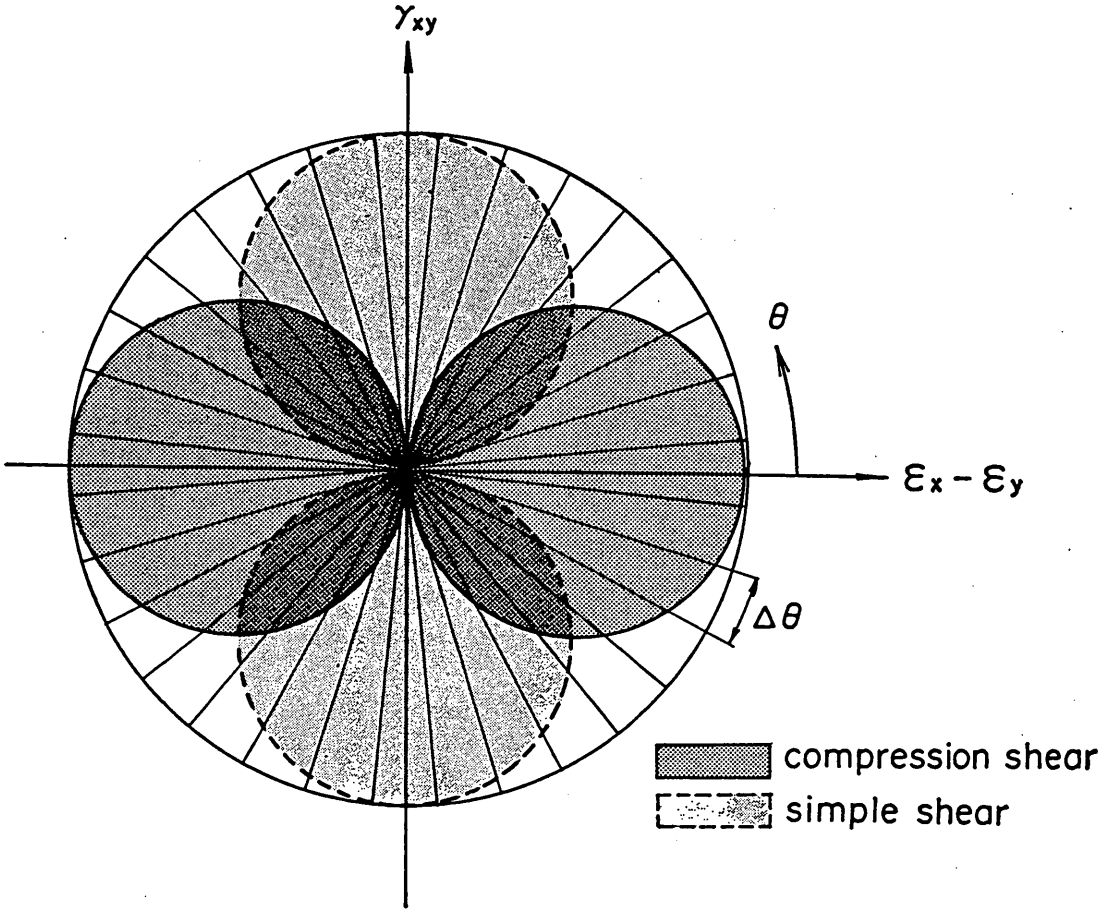

Fig. 1 Multiple simple shear mechanism
(pairs of circles indicate mobilized virtual shear strains in positive and negative modes of compression shear and simple shear)

$$\boldsymbol{n}^{(0)T}=(1,1,0) \tag{5}$$

$$\boldsymbol{n}^{(i)T}=(\cos\theta_i, -\cos\theta_i, \sin\theta_i) \qquad (\text{for } i=1,\cdots\cdots,I) \tag{6}$$

The mechanism $i=1,\cdots\cdots,I$ represents a one dimensional stress strain relation defined in a virtual simple shear which is, in concept, mobilized at angle $\theta_i/2+\pi/4$ to the x axis as shown in **Fig. 1**. The angle θ_i for mechanism i is given by

$$\theta_i=(i-1)\Delta\theta \qquad (\text{for } i=1,\cdots\cdots,I) \tag{7}$$

in which $\Delta\theta=\pi/I$. The moduli K and $R_{L/U}{}^{(i)}$ in Eq. (3) represent rebound modulus and tangent shear moduli for virtual simple shear mechanism. In particular, the rebound is given by

$$K=K_a(\sigma_m'/\sigma_{ma}')^{0.5} \tag{8}$$

in which σ_m' : effective mean stress $=(\sigma_x'+\sigma_y')/2$; K_a : elastic tangent bulk modulus of soil skeleton at $\sigma_m'=\sigma_{ma}'$; and σ_{ma}' : effective mean stress at which K is defined as $K=K_a$.

The subscript L/U for $R^{(i)}$ stands for loading/unloading and is determined for each mechanism such that, whenever $\boldsymbol{n}^{(i)T}d\boldsymbol{\varepsilon}$ changes its sige, the subscript changes from L to U or vice versa.

If the relation in Eq. (3) is more explicitly written down for practical application in mind, it is given as follows.

$$\begin{Bmatrix} d\sigma_x' \\ d\sigma_y' \\ d\tau_{xy} \end{Bmatrix} = \boldsymbol{D} \begin{Bmatrix} d\varepsilon_x \\ d\varepsilon_y \\ d\gamma_{xy} \end{Bmatrix} - \begin{Bmatrix} 1 \\ 1 \\ 0 \end{Bmatrix} K_a \left(\frac{\sigma_m'}{\sigma_{ma}'} \right)^{0.5} d\varepsilon_p \tag{9}$$

with

$$\boldsymbol{D} = K_a \left(\frac{\sigma_m'}{\sigma_{ma}'} \right)^{0.5} \begin{bmatrix} 1 & 1 & 0 \\ 1 & 1 & 0 \\ 0 & 0 & 0 \end{bmatrix} + G_{t1} \begin{bmatrix} 1 & -1 & 0 \\ -1 & 1 & 0 \\ 0 & 0 & 0 \end{bmatrix} + G_{t2} \begin{bmatrix} 0 & 0 & 1 \\ 0 & 0 & -1 \\ 1 & -1 & 0 \end{bmatrix} + G_{t3} \begin{bmatrix} 0 & 0 & 0 \\ 0 & 0 & 0 \\ 0 & 0 & 1 \end{bmatrix} \tag{10}$$

in which

$$G_{t1} = \sum_{i=1}^{I} R_{L/U}^{(i)} \cos^2\theta_i \tag{11}$$

$$G_{t2} = \sum_{i=1}^{I} R_{L/U}^{(i)} \cos\theta_i \sin\theta_i \tag{12}$$

$$G_{t3} = \sum_{i=1}^{I} R_{L/U}^{(i)} \sin^2\theta_i \tag{13}$$

The stiffness matrix $\boldsymbol{D}$ is symmetric, giving the advantage of efficient solution.

The integrated formulation corresponding to Eq. (3) is given by

$$\sigma' = -B[\varepsilon_p - (\varepsilon_x + \varepsilon_y)]^2 \boldsymbol{n}^{(0)} + \sum_{i=1}^{I} Q^{(i)}(\gamma^{(i)}) \Delta\theta \boldsymbol{n}^{(i)} \tag{14}$$

in which the function $Q^{(i)}$ is defined so that its first order derivative represents the virtual tangent shear modulus per unit angle of θ as

$$R_{L/U}^{(i)} = \frac{dQ^{(i)}}{d\gamma^{(i)}} \Delta\theta \tag{15}$$

The function $Q^{(i)}$ can be interpreted as virtual shear stress per unit angle θ for mechanism i and its value generally depends on the state as well as history of the virtual shear strain $\gamma^{(i)}$ defined by

$$\gamma^{(i)} = (\varepsilon_x - \varepsilon_y)\cos\theta_i + \gamma_{xy}\sin\theta_i \tag{16}$$

The constant B in Eq. (14) is given by

$$B = [0.5K_a/(-\sigma_{ma}')^{0.5}]^2 \tag{17}$$

2.2 Volumetric Strain of Plastic Nature

The volumetric strain of plastic nature ε_p in Eqs. (9) and (14) is given as a function of plastic shear work (Iai et al, 1990). At each stage of deformation process under transient and cyclic loads, increment in plastic shear work is computed by

$$dW_s = dW_{si} - c_1 dW_{se} \tag{18}$$

in which W_{st} : total shear work ; W_{se} : elastic shear work ; and c_1 : the parameter specifying the threshold limit in pore water pressure generation. It is understood in Eq. (18) that, if the value of right hand side should become negative, dW_s is assumed zero and a correction is applied if the effective stress is in dilative zone.

The cumulative plastic shear work W_s computed by Eq. (18) is normalized by

$$w = W_s / W_n \tag{19}$$

The factor for normalization W_n is given by

$$W_n = \tau_{m0}\gamma_{m0}/2 \tag{20}$$

in which

$$\tau_{m0} = (-\sigma_{m0}')\sin\phi_f' \tag{21}$$

$$\gamma_{m0} = \tau_{m0}/G_{m0} \tag{22}$$

$$G_{m0} = G_{ma}(\sigma_{m0}'/\sigma_{ma}')^{0.5} \tag{23}$$

with G_{ma} standing for initial shear modulus at $\sigma_{m0}' = \sigma_{ma}'$.

The normalized plastic shear work is used for computing the liquefaction front parameter by

$$S_0 = 1 - 0.6(w/w_1)^{p1} \qquad (\text{if } w < w_1)$$

$$S_0 = (0.4 - S_1)(w_1/w)^{p2} + S_1 \qquad (\text{if } w > w_1) \tag{24}$$

in which S_1, w_1, p_1 and p_2 are the material parameters which characterize the liquefaction properties of the cohesionless soil as shown in **Fig. 2.**

From the liquefaction front parameter S_0 and the deviatoric stress ratio $r = (\sigma_1' - \sigma_3')/$

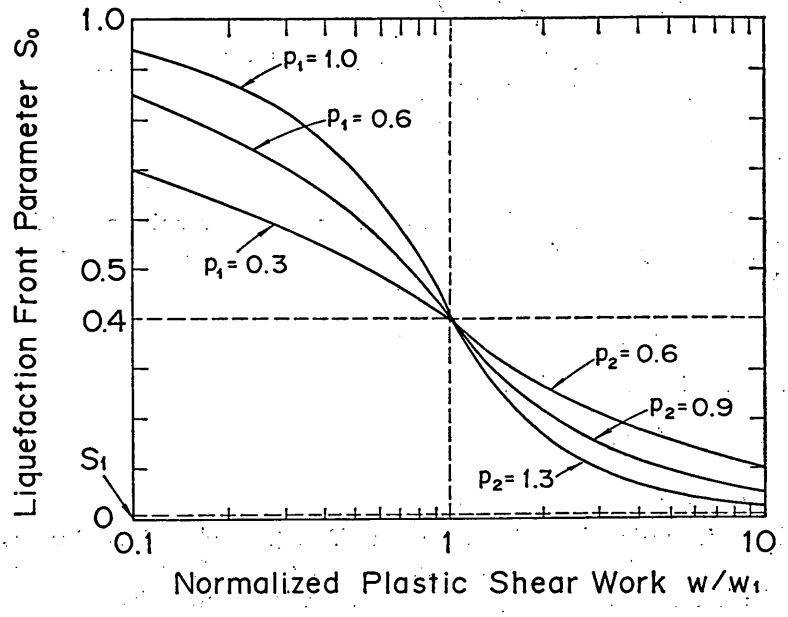

Fig. 2 Relation between normalized plastic shear work w and liquefaction front parameter S_0

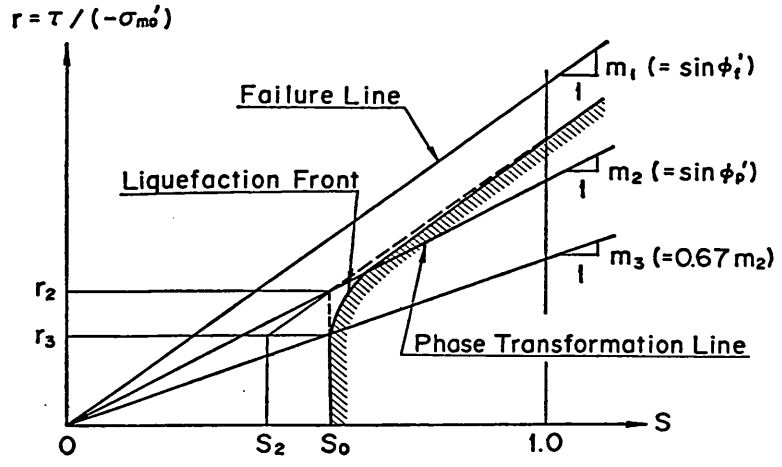

Fig. 3 Liquefaction front, state variable S and shear stress ratio r

$(-2\sigma_{m0}')$, the state variable S, which is equivalent to the effective mean stress ratio σ_m'/σ_{m0}' under constant total confining pressure, is computed, as shown in **Fig. 3**, by

$$S=S_0 \qquad \text{(if } r<r_3\text{)}$$

$$S=S_2+\sqrt{(S_0-S_2)^2+[(r-r_3)/m_1]^2} \qquad \text{(if } r>r_3\text{)} \tag{25}$$

in which

$$r_2=m_2S_0 \tag{26}$$

$$r_3=m_3S_0 \tag{27}$$

$$S_2=S_0-(r_2-r_3)/m_1 \tag{28}$$

and m_1 : inclination of failure line, defined by the shear resistance angle ϕ_f' as $m_1=\sin\phi_f'$; m_2 : inclination of phase transformation line, defined by the phase transformation angle ϕ_p' as $m_2=\sin\phi_p'$; and $m_3=0.67m_2$.

Finally, the state variable S is used for computing the volumetric strain of plastic nature by

$$\varepsilon_p=(n/K_f)(1-S)\sigma_{m0}'+[\sigma_{m0}'S/(-B)]^{0.5}+\varepsilon_{e0} \tag{29}$$

in which n and K_f are the porosity of soil skeleton and bulk modulus of water and ε_{e0} is the initial elastic volumetric strain given by

$$\varepsilon_{e0}=-[\sigma_{m0}'/(-B)]^{0.5} \tag{30}$$

This concludes the framework of strain space plasticity approach presented in the previous paper (Iai et al, 1990).

3. Modeling of Shear Mechanism

3.1 Initial Loading

In defining the virtual tangent shear moduli $R_{L/U}{}^{(i)}$ in Eq. (3) and the virtual shear stress $Q^{(i)}(\gamma^{(i)})$ in Eq. (15), it is assumed that each virtual simple shear mechanism can be approximated by the one dimensional stress strain relation observed in the actual simple shear test. With the assumption of material isotropy, $Q^{(i)}$ is given by

$$Q^{(i)}(\gamma^{(i)})=[(\gamma^{(i)}/\gamma_v)/(1+|\gamma^{(i)}/\gamma_v|)]Q_v \tag{31}$$

in which Q_v : virtual shear strength and γ_v : virtual reference strain. By substituting Eq. (31) into Eq. (15), the virtual tangent shear moduli are obtained for the initial loading as

$$R_L{}^{(i)}=[1/(1+|\gamma^{(i)}/\gamma_v|)^2](Q_v/\gamma_v)\Delta\theta \tag{32}$$

3.2 Memory of Loading History

To record the history of loading, it is postulated that the memory of loading history is registered in the normalized space defined by such variables as

$$\xi=\gamma^{(i)}/\gamma_v \tag{33}$$

$$\eta=Q^{(i)}/Q_v \tag{34}$$

In the above definition, the superscript (i) is omitted from ξ and η for simplicity but the following discussion is supposed to be applicable to each mechanism $i=1, \cdots\cdots, I$. According to this definition, the hyperbolic relation in Eq. (31) is rewritten in the normalized space as

$$\eta=\xi/(1+|\xi|) \tag{35}$$

and the curve defined by Eq. (35) in the normalized space will be called back-bone curve.

It is postulated in this study that the memory of loading history, which will affect the present and future material behavior, is completely specified by only two points out of the previous loading history defined in the normalized space; one being the point on the back-bone curve of which $|\xi|$ takes the maximum value of the previous loading history, the other being the most recent reversal point. As shown in **Fig. 4**, once unloading begins and $|\xi|$ is less than the maximum value of $|\xi|$ in the previous loading history, the point will either be directed to the memorized point on the back-bone curve or to its mirror image on the back-bone curve. When the loading continues beyond this point, the point will follow again the back-bone curve.

Thus, the formal definitions relevant to the loading processes are given as follows :

initial loading : the process which satisfies $|\xi|=\max|\xi|$
unloading/reloading : the process which satisfies $|\xi|<\max|\xi|$
  unloading : the sign of $d\xi$ is opposite to that of initial loading
  reloading : the sign of $d\xi$ is the same as that of initial loading
reversal point : a point at which $d\xi$ changes its sign

Such formal definitions can be helpful for conceptual understanding of the present approach. It is to be noted that the definitions given by $d\xi$ are consistent with the definition given earlier for subscripts L/U of $R^{(i)}$ based on the sign of $\boldsymbol{n}^{(i)T}d\varepsilon=d\xi\gamma_v$.

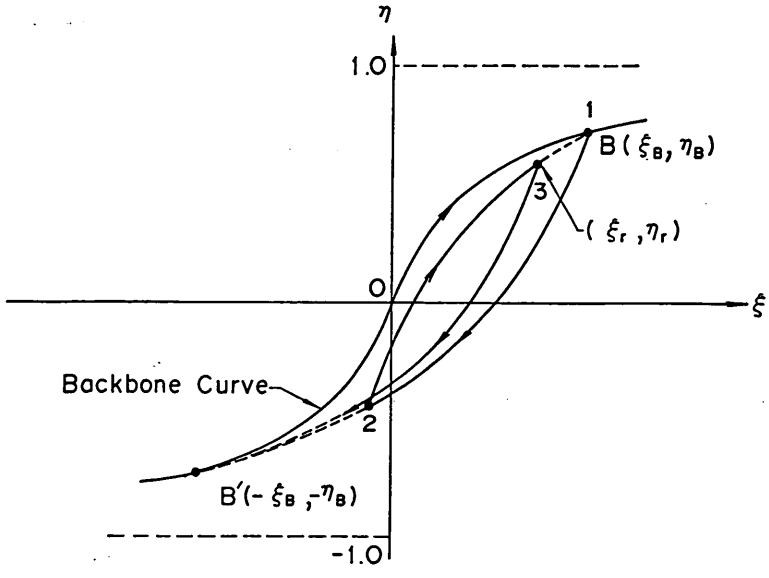

Fig. 4 Schematic figure of loading/unloading curves in the normalized space

In practice of numerical analysis, however, the following set of definitions would be much more useful;

initial loading : either of the following two;
the process which never experiences the unloading, or the process which goes beyond the previously memorized reversal point or its symmetrical image on the backbone curve

unloading/reloading : the process which begins after the reversal but which ends when the process goes either beyond the reversal point or its symmetrical image on the backbone curve.

unloading : number of the reversals is odd by counting the reversal from the back-bone curve as one

reloading : number of the reversals is even by counting the reversal from the back-bone curve as one

reversal point : a point at which not only $d\xi$ changes its sign from its previous loading process but also $d\hat{\xi}$ exceeds the threshold value δ.

The threshold value δ, similar to the small elastic region, is necessary for assuring stability in the numerical analysis; the values of the order of 10^{-6} is satisfactory in practice.

3.3 Unloading from the Initial Loading

For representing the one dimensional stress strain relation during unloading and reloading, Masing's rule was often used (Finn et al., 1977; Ishihara and Towhata, 1982); i. e. if the initial loading curve is given by

$$\eta=f(\hat{\xi}) \tag{36}$$

then the unloading and reloading curves are given by

$$(\eta-\eta_r)/2=f[(\hat{\xi}-\hat{\xi}_r)/2] \tag{37}$$

in which ξ_r and η_r represent the coordinates of the reversal point. It is known, however, that Masing's rule when combined with the hyperbolic relation does not represent the realistic hysteresis loop when the amplitude of cyclic shear strain becomes as large as a few percent; at this strain level the hysteresis loop given by Masing's rule consumes about twice the energy as those observed in the laboratory tests (Ishihara, 1982).

Such a drawback can be corrected by introducing scaling parameters into the variables ξ and η (Ishihara et al., 1985). Let us define the scaled variables by

$$\xi' = \xi / a$$
$$\eta' = \eta / b \tag{38}$$

in which the scaling parameters a and b are determined by functions of max $|\xi|$ for the previous loading history.

Let us denote the coordinates of the reversal points on the back-bone curve as ξ_B and η_B and let us scale these coordinates in the similar manner as

$$\xi_B' = \xi_B / a$$
$$\eta_B' = \eta_B / b \tag{39}$$

Using scaled coordinates in Eqs. (38) and (39), let us define a function for unloading curve from the back-bone curve by

$$(\eta' - \eta_B')/2 = f[(\xi' - \xi_B')/2] \tag{40}$$

in which

$$f(\xi) = \xi / (1 + |\xi|) \tag{41}$$

Because the curve defined by Eq. (40) shoulg do through the symmetrical image of the reversal point, one obtains

$$-\eta_B' = f(-\xi_B') \tag{42}$$

whereas the reversal point is on the back-bone curve, such that

$$\xi_B = f(\xi_B) \tag{43}$$

Elimination of η_B from Eqs. (42) and (43) by using Eqs. (39) and (41) yields

$$b = (a + |\xi_B|)/(1 + |\xi_B|) \tag{44}$$

It is to be noted that strain level of cyclic loading is represented by $|\xi_B|$, which coincides with max $|\xi|$ for the previonus loading history of transient and cyclic loading. In the following discussion $|\xi_B|$ will be conveniently called strain level. Because the scaling parameter b is determined by Eq. (44) from the parameter a and the strain level $|\xi_B|$, it remains to define a function of strain level $|\xi_B|$ for determining the scaling paramatar a.

The energy consumed by the hysteresis loop is generally expressed by a relative value to the equivalent elastic energy; a damping factor h. The definition of h is given by

$$h = (1/4\pi)(\Delta W / W) \tag{45}$$

in which ΔW is the damping energy, i. e. the area within the hysteresis loop shown in **Fig. 5**, and W is the equivalent elastic strain energy defined as

$$W = (1/2)\xi_B \eta_B \tag{46}$$

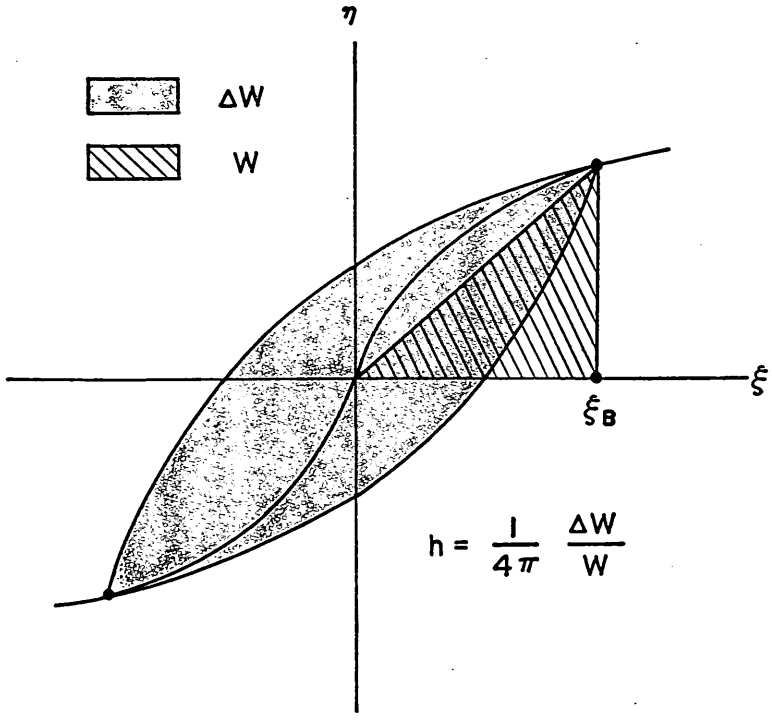

Fig. 5 Definition of damping factor h

It is to be noted that the damping factor h is independent of the normalization factors or scaling factors used for the stress and strain because effect of these factors are canceled by taking the ratio of ΔW over W in Eq. (45).

As a candidate for the realistic damping factor to be represented by each virtual simple shear mechanism, the hyperbolic function of strain level $|\xi_B|$ is adopted as

$$h(|\xi_B|)=[|\xi_B/\xi_h|/(1+|\xi_B/\xi_h|)]h_v \tag{47}$$

in which h_v : limiting value of virtual damping factor when virtual shear strain level is infinity; and ξ_h a parameter similar to virtual reference strain.

Because the hysteresis loop defined by Eq. (40) produces the damping factor D as (Ishihara, 1982)

$$D(|\xi'_B|)=(4/\pi)(1+1/|\xi'_B|)[1-(1/|\xi'_B|)]\ln(1+|\xi'_B|)-(2/\pi) \tag{48}$$

the scaling parameter a should be determined so as to produce the same value for D and h for and same strain level $|\xi_B|$ such that

$$D(|\xi_B/a|)=h(|\xi_B|) \tag{49}$$

Once unloading begins from the back-bone curve at the virtual normalized shear strain ξ_B, the scaling parameter a is determined by numerically solving Eq. (49) from the current strain level $|\xi_B|$. Then, the corresponding scaling parameter b is determined by Eq. (44) and consequently the unloading curve is given by Eq. (40).

The unloading curve in Eq. (40) can be more explicitly written by converting the normalized variables ξ' and η' to the original variables $\gamma^{(i)}$ and $Q^{(i)}$, such that

$$(Q^{(i)}/Q_v-\eta_B)/(2b)=f[(\gamma^{(i)}/\gamma_v-\xi_B)/(2b)] \tag{50}$$

in which the function f is defined by Eq. (41) and ξ_B, η_B, a and b are, as mentioned earlier, separately defined for each mechanism $i=1, \cdots\cdots, I$.

By substituting Eq. (50) into Eq. (15), the virtual tangent shear moduli are obtained for the unloading from the initial loading as

$$R_U{}^{(i)}=g[(\gamma^{(i)}/\gamma_v-\xi_B)/(2a)](Q_v/\gamma_v)(b/a)\Delta\theta \tag{51}$$

in which the function g is the first order derivative of f in Eq. (41) and given by

$$g(\xi)=1/(1+|\xi|)^2 \tag{52}$$

3. 4 Reloading

For representing the one dimensional stress strain relation during reloading and re-unloading, a function similar to Eq. (40) is used for interpolation between the most recent reversal point (ξ_r, η_r) at which the current reloading or re-unloading process initiated and the most recent reversal point or its symmetrical image on the back-bone curve to which the current process is directed. The function is given by

$$(\eta'-\eta_r')/(2c)=f[(\xi'-\xi_r')/(2c)] \tag{53}$$

The scaling factor c is determined so that the curve defined by Eq. (53) goes through the most recent reversal point or its symmetrical image on the back-bone curve, such that

$$(\pm\eta_B'-\eta_r')/(2c)=f[(\pm\xi_B'-\xi_r')/(2c)] \tag{54}$$

in which $\pm$ takes plus if reloading and minus if re-unloading. By solving Eq. (54) for c with the help of Eq. (41), one obtains

$$c=(1/2)|\pm\xi_B'-\xi_r'|(\pm\eta_B'-\eta_r')/[(\pm\xi_B'-\xi_r')-(\pm\eta_B'-\eta_r')] \tag{55}$$

Explicit equations for $Q^{(i)}$ and $R_{L/U}{}^{(i)}$ similar to Eqs. (50) and (51) will be obtained if the scaling factors ac and bc are used on behalf of a and b in these equations and the coordinates of reversal point ξ_r and η_r are used on behalf of ξ_B and η_B. Thus, for reloading and re-unloading

$$(Q^{(i)}/Q_v-\eta_r)/(2bc)=f[(\gamma^{(i)}/\gamma_v-\xi_r)/(2ac)] \tag{56}$$

$$R_{L/U}{}^{(i)}=g[(\gamma^{(i)}/\gamma_v-\xi_r)/(2ac)](Q_v/\gamma_v)(b/a)\Delta\theta \tag{57}$$

As mentioned earlier, ξ_r, η_r, a, b and c are separately defined for each mechanism $i=1, \cdots\cdots, I$.

4. Parameter Identification for Shear Mechanism

In the previous chapter, four soil parameters are introduced for modeling shear mechanism; the virtual shear strength Q_v and the virtual reference strain γ_v in Eq. (31), and the limiting value of virtual damping factor h_v and a parameter ξ_h in Eq. (47). Though these parameters are not directly measurable, they can be readily determined from the well defined soil parameters which are measurable in the laboratery test.

4. 1 Virtual Shear Strength and Virtual Reference Strain

The virtual shear strength and the virtual reference strain in Eqs. (31) and (32) can be readily determined by such measurable parameters as shear strength τ_m and shear modulus G_m at small strain level. Following the approach by Towhata and Ishihara (1985), let us consider a simple shear test under drained and monotonic loading. It is assumed that only non zero shear strain is γ_{xy}. When the shear strain is very small such as $\gamma_{xy}=0$, definition of shear modulus G_m implies

$$d\tau_{xy}=G_m d\gamma_{xy} \tag{58}$$

whereas Eq. (32) yields

$$R_L{}^{(i)}=(Q_v/\gamma_v)\Delta\theta \tag{59}$$

Substitution of Eq. (59) into Eq. (11) through (13) yield

$$G_{t2}=0$$

$$G_{t3}=(Q_v/\gamma_v)\sum_{i=1}^{I}\sin^2\theta_i\Delta\theta \tag{60}$$

and, therefore, Eqs. (9) and (10) yield

$$d\tau_{xy}=[(Q_v/\gamma_v)\sum_{i=1}^{I}\sin^2\theta_i\Delta\theta]d\gamma_{xy} \tag{61}$$

By comparing Eqs. (58) and (61), one obtains

$$G_m=(Q_v/\gamma_v)\sum_{i=1}^{I}\sin^2\theta_i\Delta\theta \tag{62}$$

Similarly, when $\gamma_{xy}=\infty$, definition of shear strength τ_m implies

$$\tau_{xy}=\tau_m \tag{63}$$

whereas Eq. (31) yields

$$Q^{(i)}(\infty)=Q_v \tag{64}$$

Substitution of Eq. (64) into Eq. (14) yields

$$\tau_{xy}=Q_v\sum_{i=1}^{I}\sin\theta_i\Delta\theta \tag{65}$$

By comparing Eqs. (63) and (65), one obtains

$$\tau_m=Q_v\sum_{i=1}^{I}\sin\theta_i\Delta\theta \tag{66}$$

From Eqs. (62) and (66), the virtual shear strength and reference strain are determined as

$$Q_v=\tau_m/\left(\sum_{i=1}^{I}\sin\theta_i\Delta\theta\right) \tag{67}$$

$$\gamma_v=(Q_v/G_m)\sum_{i=1}^{I}\sin^2\theta_i\Delta\theta \tag{68}$$

When the number of multiple mechanisms are increased to infinity, the limiting value in Eqs. (67) and (68) will be given as

$$Q_v^{\infty}=\tau_m/2 \tag{69}$$

$$\gamma_v^{\infty}=(\pi/2)(Q_v/G_m) \tag{70}$$

The relations in Eqs. (69) and (70) are consistent with the results obtained by Towhata and Ishihara (1985).

4. 2 Parameters Relevant to Hysteresis Loop

The soil parameters h_v and ξ_h for virtual simple shear mechanism in Ep. (47) can be readily determined by such a measurable parameter as damping factor of actual simple shear. Let us examine the behavior of virtual shear mechanisms during the actual cyclic simple shear under drained condition. The amplitude of the shear strain will be denoted γ_{xyB}. When unloading starts at the peak value,

$$\gamma_{xy}=\gamma_{xyB} \tag{71}$$

so that the virtual simple shear strain amplitude is given by Eq. (16) as

$$\gamma^{(i)}{}_B=\gamma_{xyB}\sin\theta_i \tag{72}$$

and the corresponding virtual simple shear stress are given by Eq. (31) as

$$Q^{(i)}{}_B=Q^{(i)}(\gamma^{(i)}{}_B) \tag{73}$$

From this and Eq. (14), the actual simple shear stress amplitude is given by

$$\tau_{xyB}=\sum_{i=1}^{I}Q^{(i)}{}_B\sin\theta_i\Delta\theta \tag{74}$$

Therefore, the equivalent strain energy for the cyclic loading process of shear strain amplitude γ_{xyB} is given by

$$W=(1/2)\left[\sum_{i=1}^{I}Q^{(i)}{}_B\sin\theta_i\Delta\theta\right]\gamma_{xyB} \tag{75}$$

By rearranging this and using Eq. (72), one obtains

$$W=(1/2)\sum_{i=1}^{I}Q^{(i)}{}_B\gamma^{(i)}{}_B\Delta\theta \tag{76}$$

If the equivalent elastic virtual strain energy is defined as

$$W^{(i)}=(1/2)Q^{(i)}{}_B\gamma^{(i)}{}_B \tag{77}$$

the equivalent elastic strain energy in Eq. (76) is rewritten as

$$W=\sum_{i=1}^{I}W^{(i)}\Delta\theta \tag{78}$$

Thus, the equivalent elastic strain energy is obtained by summing up the equivalent elastic virtual strain energy.

Similarly, the energy consumed by the actual hysteresis loop ΔW is given by summing up the energy consumed by each stress contribution appearing in the right hand side of Eq. (74). In order to do the summation, some elaboration is necessary. First of all, let us go back to the definition of damping factor in Eq. (45) and write down the explicit equation for the damping energy ΔW. As mentioned before, the damping factor is defined irrespective of the scaling factors for the relevant variables. Since the area within the hysteresis loop (in the actual stress and strain space) is twice the upper half of the area, one

obtains

$$\Delta W=2\int_{-|\gamma_{xyB}|}^{|\gamma_{xyB}|}[\tau_{xy}-(\tau_{xyB}/\gamma_{xyB})\gamma_{xy}]d\gamma_{xy} \tag{79}$$

The linear term in the integral will vanish upon integration so that

$$\Delta W=2\int_{-|\gamma_{xyB}|}^{|\gamma_{xyB}|}\tau_{xy}d\gamma_{xy} \tag{80}$$

In the manner similar to the derivation of Eqs. (72) through (74), τ_{xy} is expressed by the virtual simple stress $Q^{(i)}$ as

$$\tau_{xy}=\sum_{i=1}^{I}Q^{(i)}\sin\theta_i\Delta\theta \tag{81}$$

in whicn

$$Q^{(i)}=Q^{(i)}(\gamma^{(i)}) \tag{82}$$

$$\gamma^{(i)}=\gamma_{xy}\sin\theta_i \tag{83}$$

Substitution of Eq. (81) into Eq. (80) yields

$$\Delta W=2\int_{-|\gamma_{xyB}|}^{|\gamma_{xyB}|}[\sum_{i=1}^{I}Q^{(i)}\sin\theta_i\Delta\theta]d\gamma_{xy} \tag{84}$$

By rearranging this, one obtains

$$\Delta W=2\sum_{i=1}^{I}\left[\int_{-|\gamma_{xyB}|}^{|\gamma_{xyB}|}Q^{(i)}d\gamma_{xy}\sin\theta_i\Delta\theta\right] \tag{85}$$

The transformation of the variable for the integration from γ_{xy} to $\gamma^{(i)}=\gamma_{xy}\sin\theta_i$ in Eq. (85) yields

$$\Delta W=2\sum_{i=1}^{I}\left[\int_{-|\gamma^{(i)}{}_B|}^{|\gamma^{(i)}{}_B|}Q^{(i)}d\gamma^{(i)}\right]\Delta\theta \tag{86}$$

If, by the analogy to Eq. (80), the consumed energy by each virtual simple shear mechanism is defined as

$$\Delta W^{(i)}=2\int_{-|\gamma^{(i)}{}_B|}^{|\gamma^{(i)}{}_B|}Q^{(i)}d\gamma^{(i)} \tag{87}$$

Eq. (86) will be rewritten as

$$\Delta W=\sum_{i=1}^{I}\Delta W^{(i)}\Delta\theta \tag{88}$$

Thus, the energy consumed by the actual hysteresis loop is given by summing up the energy

consumed by each virtual simple shear mechanism.

It remains to identify $\Delta W^{(i)}$ with the damping factor h defined in Eq. (45) for virtual simple shear mechanism. Since the damping factor h defined in Eq. (45) is irrespective of the scaling factors for the relevant variables, the damping factor h is equal to the ratio of the energies $\Delta W^{(i)}$ over $W^{(i)}$ defined by the variables with $\gamma^{(i)}$ and $Q^{(i)}$, such that

$$h(|\gamma_B{}^{(i)}/\gamma_v|) = (1/4\pi)(\Delta W^{(i)}/W^{(i)}) \tag{89}$$

in which $W^{(i)}$ and $\Delta W^{(i)}$ are defined in Eqs. (77) and (87). Therefore, $\Delta W^{(i)}$ is determined from h and $W^{(i)}$ as

$$\Delta W^{(i)} = 4\pi h(|\gamma_B{}^{(i)}/\gamma_v|)\, W^{(i)} \tag{90}$$

Substitution of Eq. (90) into Eq. (88) yields

$$\Delta W = 4\pi \sum_{i=1}^{I} h(|\gamma_B{}^{(i)}/\gamma_v|)\, W^{(i)} \Delta\theta \tag{91}$$

From Eqs. (78) and (91), one finally obtains the damping factor for the actual simple shear as

$$H(|\gamma_{xyB}|) = \left[\sum_{i=1}^{I} W^{(i)} h(|\gamma^{(i)}{}_B/\gamma_v|)\right] \Big/ \left[\sum_{i=1}^{I} W^{(i)}\right] \tag{92}$$

in which $W^{(i)}$ and $\gamma^{(i)}{}_B$ are defined by Eqs. (77) and (72).

Whereas the damping factor given by the present model is thus identified, the actual damping factor to be measured in the laboratory is postulated to be given by the hyperbolic relation proposed by Hardin and Drnevich (1972), such that

$$\tilde{H}(|\gamma_{xyB}|) = [|\gamma_{xyB}/\gamma_m|/(1+|\gamma_{xyB}/\gamma_m|)]H_m \tag{93}$$

in which H_m is damping factor when the shear strain amplitude is infinity and γ_m is reference strain defened by

$$\gamma_m = \tau_m/G_m \tag{94}$$

From these measurable parameters H_m and γ_m, the parameters h_v and ξ_h for the virtual shear are determined as follows. First of all, when $|\gamma_{xyB}|$ becomes infinity, damping factor given by Eq. (92) becomes

$$H(\infty) = h_v \tag{95}$$

From this and Eq. (93), one obtains

$$h_v = H_m \tag{96}$$

The parameter ξ_h similar to virttual reference strain is numerically determined so that H is best fitted to $\tilde{H}$.

To summarize the discussions presented in this chapter, the shear mechanism is completely defined by three soil parameters : i. e. the shear modulus at small strain level, the shear strength and the damping factor at large shear strain. Once initial values are given by Eqs. (21) through (23) with the damping factor at large shear strain, the soil parameters τ_m, G_m and γ_m during cyclic mobility are given as a function of current value of effective mean stress as well as the liquefaction front parameter S_0 by a scheme for enhancing the numerical robustness and efficiency (Iai et al., 1990).

5. Parameter Identification for Volumetric Mechanism

In addition to three parameters for the shear mechanism G_{ma}, ϕ_f', H_m in Eq. (21), (23), and (93), there are five parameters to be specified for the present model; i. e. S_1, w_1, p_1, p_2, and c_1 in Eqs. (18) and (24) through (28). Though there are four more parameters such as phase transformation angle ϕ_p', bulk moduli of soil skeleton and water K_{ma} and K_f and porosity of soil skeleton n, they are so well defined that no more explanation would be necessary. Given the soil parameters for shear mechanism G_{ma}, ϕ_f', H_m as well as the well defined parameters ϕ_p', K_{ma}, K_f and n, the five parameters S_1, w_1, p_1, p_2 and c_1 for defining the cumulative volumetric strain of plastic nature are determined from the undrained cyclic loading test results as follows.

1) First of all, the test data, commonly available in the practice of soil dynamics, should be provided for representing (i) liquefaction resistance curve (i. e. the cyclic shear stress ratio vs. number of the cyclie loading N_l required to cause shear strain of 5 percent in the double amplitude), (ii) envelope of excess pore water pressure generation curve as shown in **Fig. 6** by a broken line and (iii) envelope of shear strain amplitude as shown in **Fig. 7** by broken lines.
2) S_1 takes small positive value about 0.005 so that S_0 will never be zero. In such a special case as the stress strain curve should become a closed loop during cyclic mobility, S_1 can take a larger value and can be determined in a try and error manner.
3) The parameter c_1 for specifying the threshold level is temporarily fixed to 1.0 as a first guess. The value of c_1 will later be modified in a try and error manner. The modification in the value of c_1, however, does not have a great influence upon the cyclic

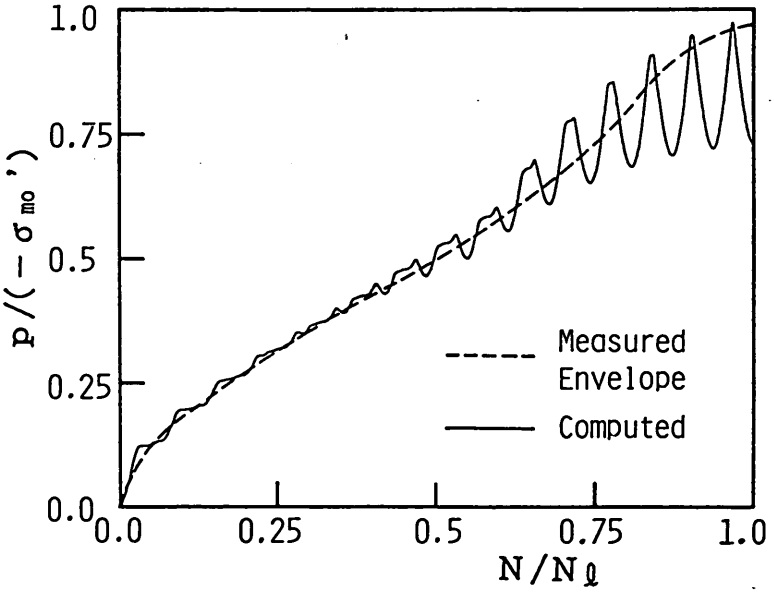

Fig. 6 Excess pore water pressure generation curve

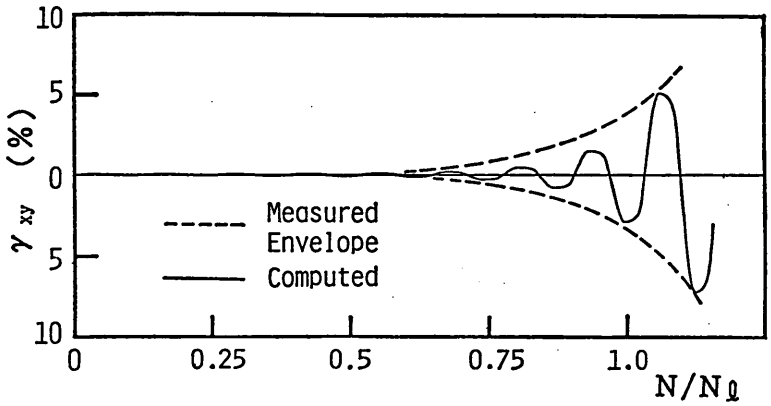

Fig. 7 Shear strain amplitude

mobility when the shear stress ratio is much larger than the threshold level. Therefore, with $c_1=1.0$, the rest of the parameters w_1, p_1 and p_2 are determined from the test results of reletively large shear stress ratio by the following steps.

4) The parameters w_1 and p_1 are determined in a try and error manner from the excess pore water pressure generation curve. In particular, the portion of the curve for $p/(-\sigma_{m0}')<0.6$ is used, in which p denotes excess pore water pressure. Because w_1 is not greatly influenced by the variation in p_1, the parameter w_1 is at first determined with appropriate guess of p_1. The value of p_1 ranges from about 0.4 to 0.7. With the determined value of w_1, the value of p_1 is determined. In general the greater w_1 is and the greater p_1 is, the slower the pore water pressure rises.

5) The parameter p_2 could also be determined from the pore water pressure generation curve for $p/(-\sigma_{m0}')>0.6$. However, it is better to determine the parameter p_2 from the envelope of strain amplituda if the primary purpose of the cyclic mobility analysis is to estimate the amount of deformation in the soil structures and foundations. The value of p_2 ranges from about 0.6 to 1.5; the greater p_2 is, the faster the shear strain amplitude increases.

6) When all the parameters are determined by the steps mentioned above from the laboratory data at relatively large shear stress ratio, the next step is to examine if these parameters are appropriate for representing the laboratory data at relatively small shear stress ratio. If not, then the parameter c_1 is modified in a try and error manner.

6. Model Performance

As an example, the model parameters are determined by using the laboratory data of Fuji River Sand at relative density of 47% presented by Ishihara (1985). With the model parameters shown in **Table 1**, the model gives the computed results shown by solid lines in **Figs. 6** and **7**. Reasonable adaptability to the soil behavior in the laboratory is indicated by these results. Model performance in representing the effective stress path and the stress strain curve are shown somewhere else (Iai et al., 1990).

These results are obtained with the initially isotropically consolidated condition. In order to examine the effect of initial K_0 consolidation, the undrained torsion shear tests is simulated with initially $K_0=0.5$ but with constraining the bulging. The same parameters

Table 1 Model parameters

Parameters	Loose Fuji River Sand (D_r=47%)	Dense Fuji River Sand (D_r=75%)
K_{ma}	270500 kPa	366800 kPa
G_{ma}	103700 kPa	140700 kPa
p_1	0.45	0.40
p_2	1.4	0.72
w_1	2.0	2.85
S_1	0.0035	0.005
c_1	1.0	1.0
$\sin\phi_f'$	0.87	0.91
$\sin\phi_p'$	0.42	0.42
H_m	0.3	0.3
n	0.45	0.40
K_f	2.0×10^6 kPa	2.0×10^6 kPa

K_{ma} and G_{ma} are given for $(-\sigma_{ma}')$=98 kPa. The computation was done with number of the shear mechanism I=12 by 50 steps of incremental loadings for 1/4 cycle.

for the looser sand in **Table 1** and the same initial confining pressure are used for the computation. The result, shown in **Fig. 8**, indicates that (1) stress strain relation is similar to that in the initially isotropically consoldated sand (if compared with **Fig. 9** in Iai et al., 1990) and (2) initial deviatoric stress due to K_0 consolidation is gradually released as the cyclic loading continues. If the shear stress ratio, i. e. the ratio of the cyclic shear stress over the initial confining pressure, is plotted with number of the cyclic loading required to cause shear strain of 5 percent in the double amplitude, the computed result on the isotropically consol-

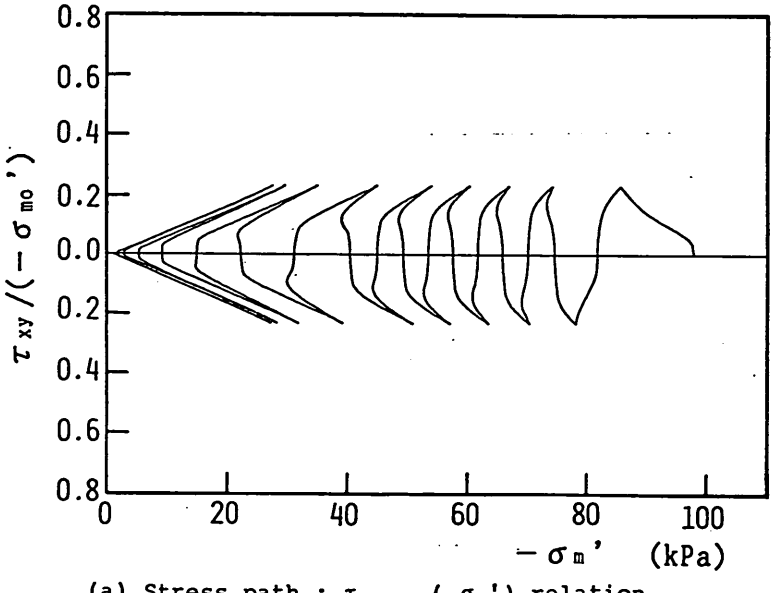

(a) Stress path : τ_{xy} - $(-\sigma_m')$ relation

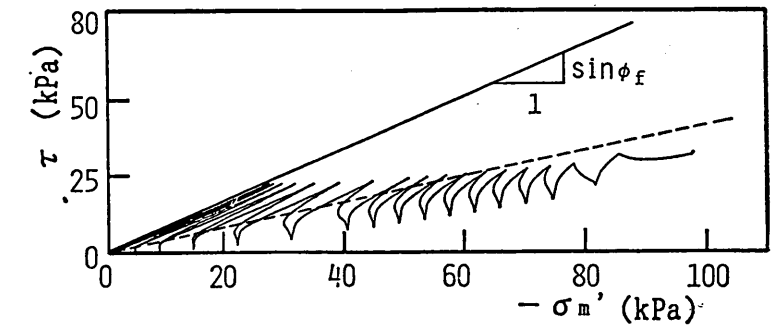

(b) Stress path : $\tau=(\sigma_1'-\sigma_3')/2$ - $(-\sigma_m')$ relation

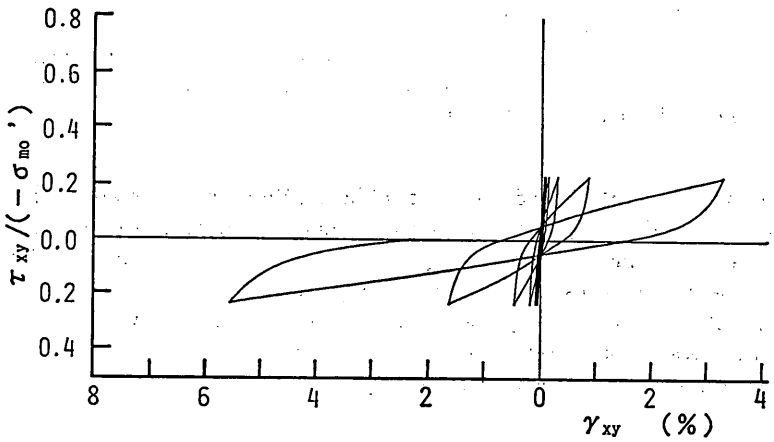

(c) Stress strain curve

Fig. 8 Computed results of loose sand on K_0 consolidated soil with $K_0=0.5$ (bulging constrained)

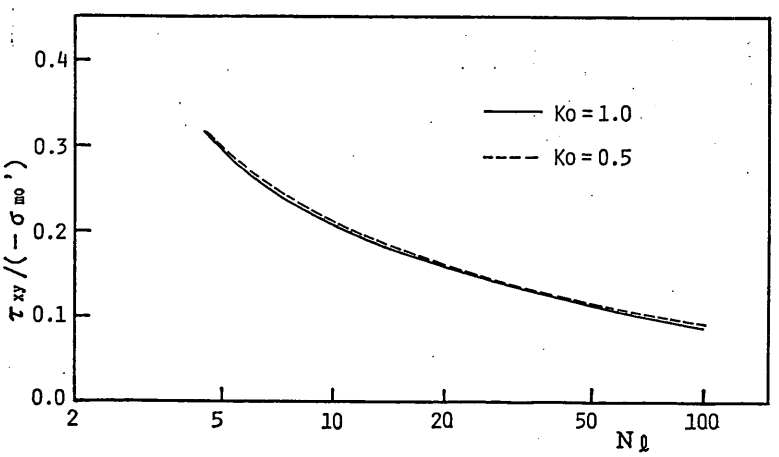

Fig. 9 Comparison of liquefaction resistances between isotropically and K_0 consolidated soils

idated sand agrees with that on the K_0 consolidated sand as shown in **Fig. 9.** This is consistent with the results by the laboratory study (Ishihara, et al., 1977).

The model performance examined above is closely related with the one dimensional analysis of cyclic mobility in the level ground in which the bulging of soil is constrained. When the two dimensional analysis is conducted for such soil structures as embankment, initial stress due to gravity will act as a driving force for the gradual settlement and bulging. In order to examine the ability to simulate such a mechanism, undrained torsion shear test with initially K_0 consolidated sand is simulated with keeping the initial normal stress difference unchanged as the stress boundary condition. The results, as shown in **Fig. 10,** indicate the limit in decreasing value of $(-\sigma_m')$ and the gradual settlement with bulging of soil element (i. e. gradual increase in $\varepsilon_x - \varepsilon_y$), suggesting reasonable applicability in the two dimensional analysis.

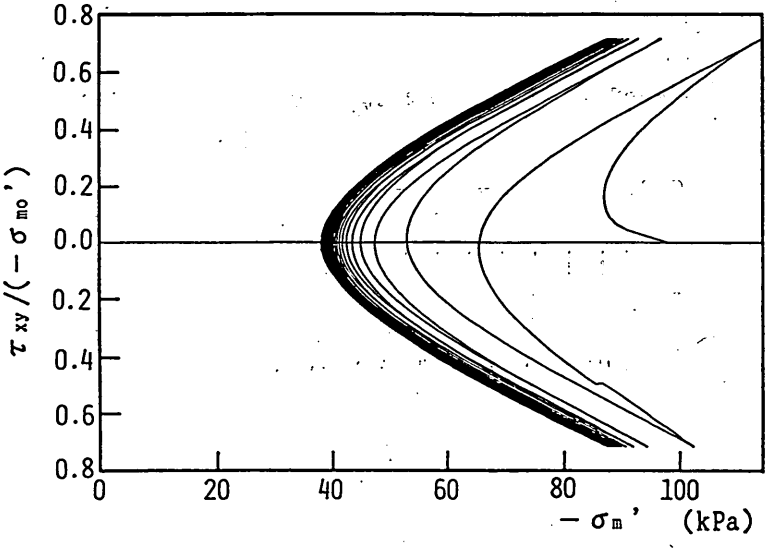

(a) Stress path : τ_{xy} - $(-\sigma_m')$ relation

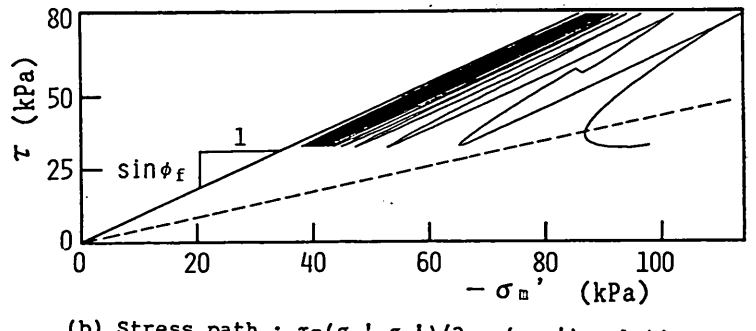

(b) Stress path : $\tau=(\sigma_1'-\sigma_3')/2$ - $(-\sigma_m')$ relation

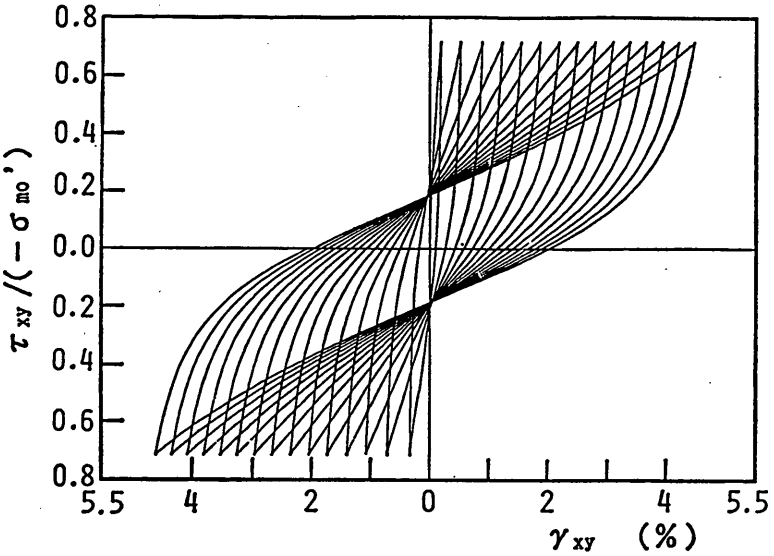

(c) Stress strain curve : $\tau_{xy}/(-\sigma_{m0}')$ - γ_{xy} relation

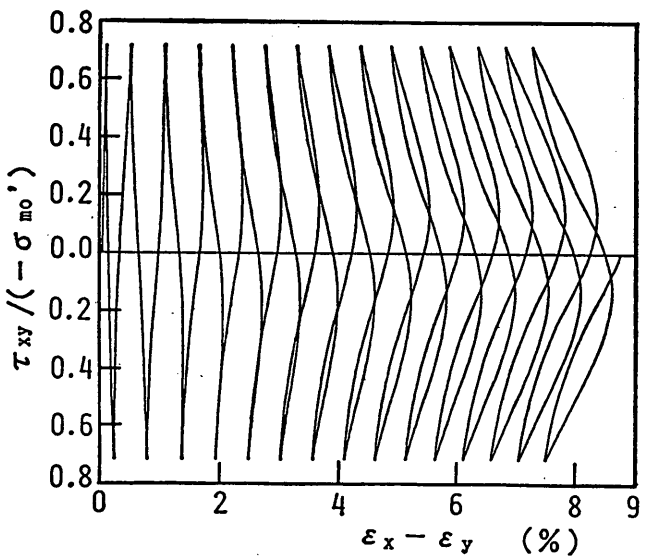

(d) Stress strain curve : $\tau_{xy}/(-\sigma_{m0}')$ - $(\varepsilon_x-\varepsilon_y)$ relation

Fig. 10 Computed results of dense sand and on K_0 consolidated soil with $K_0=0.5$ under constant normal stress difference boundary conditions (bulging unconstrained)

7. Conclusions

In order to represent the realistic damping factor during cyclic loadig, such a conventional tool as Masing's rule is not applicable in large shear strain level. This study shows how to represent the realistic damping factor in the framework of strain space plasticity approach. The framework is used for decomposing the shear mechanism into a set of virtual simple shear mechanisms. The virtual damping factor in the virtual simple shear mechanism is adjusted by introducing appropriate scaling factors for virtual strain and stress.

The parameters introduced for the virtual simple shear mechanism are identified with three measurable soil parameters; i. e. the shear strength, the shear modulus at small strain level and damping factor at large shear strain level.

The rest of five parameters for defining the cumulative volumetric strain of plastic nature are identified with the undrained cyclic loading test data. The reasonable adaptability of the proposed model is indicated.

(Received on September 29, 1990)

Acknowledgments

The authors with to thank Professors K. Ishihara and I. Towhata at Tokyo University for their valuable discussions and encouragements.

References

1) Finn, W. D. L., Lee, K. W. and Martin, G. R. (1977) : "An effectie stress model for liquefaction," *Journal of the Geotechnical Engineering Division*, ASCE, Vol. 103, No. GT6, pp. 517-533.
2) Hardin, B. O. and Drnevich, V. P. (1972) : "Shear modulus and damping of soils : design equation and curves," *Journal of Soil Mechanics and Foundation Division*, ASCE, Vol. 98, No. SM7, pp. 667-692.
3) Iai, S., Matsunaga, Y. and Kameoka, T. (1990) : "Strain space plasticity model for cyclic mobility," *Report of Port and Harbour Research Institute*, Vol. 29, No. 4
4) Ishihara, K. (1982) : "Evaluation of soil properties for use in earthquake response analysis," *Proceedings of International Symposium on Numerical Models in Geomechanics*, Zurich, pp. 237-257
5) Ishihara, K. (1985) : "Stability of natural deposits during earthquakes," *Proceedings of 11th International Conference on Soil Mechanics and Foundation Engineering*, San Francisco, Vol. 1, pp. 327-376
6) Ishihara, K., Iwamoto, S., Yasuda, S. and Takatsu, H. (1977) : "Liquefaction of anisotropically consolidated sand," *Proceedings of 9th International Conference on Soil Mechanics and Foundation Engineering*, Tokyo, Vol. 2, pp. 261-264
7) Ishihara, K. and Towhata, I. (1982) : "Dynamic response analysis of level ground based on the effective stress method," Pande, G. N. and Zienkiewicz, O. C. (eds.), *Soil Mechanics-Transient and Cyclic Loads*, Chapter 7, John Wiley and Sons, pp. 133-172
8) Ishihara, K., Yoshida, N. and Tsujino, S. (1985) : "Modelling of stress-strain relations of

soils in cyclic loading," *Proceedings of 5th Conference on Numerical Methods in Geomechanics*, Nagoya, Vol. 1, pp. 373-380

9) Towhata, I. and Ishihara, K. (1985) : "Modelling soil behaviour under principal stress axes rotation," *Proceedings of 5th International Conference on Numerical Methods in Geomechanics*, Nagoya, Vol. 1, pp. 523-530

Notation

a, b and c : scaling parameters for virtual simple shear mechanism
$B=[0.5K_a/(-\sigma_{ma}')^{0.5}]^2$: factor for volumetric relation
c_1 : parameter for specifying the level of threshold limit
$\boldsymbol{D}$: tangential stiffness matrix
D : damping factor given by Masing's rule with hyperbolic relation
f and g : normalized hyperbolic relation and its tangent stiffness
G_{mo} : initial shear modulus
G_m : shear modulus
G_{t1}, G_{t2} and G_{t3} : factors for tangent stiffness
H : damping factor generated by the present model
$\tilde{H}$: damping factor given by hyperbolic relation
H_m : limiting value of damping factor
h : damping factor for virtual simple shear
h_v : limiting value of virtual damping factor
I : number of the multiple mechanism for shear
K : elastic tangent bulk modulus of soil skeleton
K_a : value of K at $\sigma_m'=\sigma_{ma}'$
K_f : bulk modulus of pore water
$m_1=\sin\phi_f'$: inclination of failure line
$m_2=\sin\phi_p'$: inclination of phase transformation line
$m_3=0.67m_2$: auxiliary parameter
$\boldsymbol{n}^{(i)}$: loading/unloading direction vector for mechanism i
n : porosity of soil skeleton
p_1, p_2, w_1, S_1 : material parameters for dilatancy
$Q^{(i)}$: virtual shear stress per unit angle for mechanism i
$Q^{(i)}{}_B$: virtual simple shear stress amplitude per unit angle
Q_v : virtual shear strength per unit angle
r : state variable equivalent to $\tau/(-\sigma_{m0}')$
$R_{L/U}{}^{(i)}$: tangential stiffness modulus of mechanism i at loading and unloading
S : state variable equivalent to σ_m'/σ_{m0}'
S_0 : liquefaction front parameter
W : equivalent elastic strain energy
ΔW : damping energy of hysteresis loop
W_n : factor for normalization of shear work
W_s : plastic shear work
W_{st} : total shear work
W_{se} : elastic shear work
$W^{(i)}$: equivalent elastic virtual strain energy for mechanism i
$\Delta W^{(i)}$: damping energy in virtual mechanism for hysteresis loop
w : normalized shear work
$\gamma^{(i)}$: virtual simple shear strain for mechanism i

γ_{m0} : initial reference strain
γ_m : reference strain
γ_v : virtual reference strain
γ_{xyB} : amplitude of simple shear strain
$\gamma^{(i)}{}_B$: amplitude of virtual simple shear strain for mechanism i
$\varepsilon^T=(\varepsilon_x,\ \varepsilon_y,\ \gamma_{xy})$: strain
ε_p : additional volumetric strain of plastic nature
ε_{e0} : initial elastic volumetric strain
$\theta_i=(i-1)\Delta\theta$: angle for virtual shear mechanism i in $(\varepsilon_x-\varepsilon_y)-\gamma_{xy}$ plane
$\Delta\theta=\pi/I$
ξ_h : a parameter for damping factor similar to virtual reference strain
$\xi,\ \eta$: normalized virtual strain and stress
$\xi',\ \eta'$: normalized and scaled virtual strain and stress
$\xi_B,\ \eta_B$: coordinates of reversal point on the back-bone curve
$\xi_r,\ \eta_r$: coordinates of reversal point
$\sigma'^T=(\sigma_x',\ \sigma_y',\ \tau_{xy})$: effective stress
$\sigma_m'=(\sigma_x'+\sigma_y')/2$: mean effective stress
σ_{m0}' : initial mean effective stress
$\tau=(\sigma_1'-\sigma_3')/2$: deviatoric stress
τ_m : shear strength
τ_{m0} : initial shear strength
ϕ_f' : shear resistance angle
ϕ_p' : phase transformation angle